PROCEEDINGS OF SCIENCE

Modelling Optical Emission and Polarization of Relativistic AGN Jets Using RMHD Simulations.

Reuben Immelman,[1,*] **Izak P. van der Westhuizen,**[1] **Brian van Soelen,**[1] **Jacques Maritz**[2] **and Bhargav Vaidya**[3]

[1]*Department of Physics, University of the Free State, 9300, Bloemfontein, South Africa.*
[2]*Department of Engineering Sciences, University of the Free State, 9300, Bloemfontein, South Africa.*
[3]*Discipline of Astronomy, Astrophysics and Space Engineering, Indian Institute of Technology Indore, Khandwa Road, Simrol, Indore, 453552, India.*
E-mail: immelmanr@ufs.ac.za, VanDerWesthuizenIP@ufs.ac.za, vansoelenb@ufs.ac.za, MaritzJM@ufs.ac.za, bvaidya@iiti.ac.in

Radio-loud Active Galactic Nuclei (AGN) exhibit non-thermal emission observed to span the entire electromagnetic spectrum. The majority of the emission at lower energies (from radio to soft X-rays) is produced by synchrotron emission of non-thermal electrons within a relativistic jet. The structure and kinematics of these relativistic jets can be simulated using relativistic magneto-hydrodynamic (RMHD) simulations. A 3D RMHD simulation was set up with the PLUTO code that consisted of a uniform background medium with a less dense jet. A domain size of 5 pc was used to model the sub-parsec region. The jet was separated into two regions, namely the spine (the inner region of the jet) and the sheath (the outer region of the jet). The spine had a radius of 0.033 pc and a maximum bulk Lorentz factor of $\Gamma_{\rm max} = 10$, while the sheath had a radius of 0.1 pc and a maximum bulk Lorentz factor of $\Gamma_{\rm max} = 3$. A helical magnetic field orientation was utilized where the spine and sheath had a maximum magnetic field magnitude of $B = 50$ mG and $B = 5$ mG, respectively. Lagrangian particles were injected at the base of the jet with an initial power-law distribution, and were allowed to evolve with time. The synchrotron and linear polarization emission coefficients were then integrated along a user defined line of sight to produce the I, Q and U Stokes parameters. We present the initial results from this study showing the spectral energy distribution (SED) and wavelength dependent polarization.

High Energy Astrophysics in Southern Africa (HEASA)
5-9 September, 2023
Mtunzini, Kwa-Zulu Natal, South Africa

*Speaker

PoS(HEASA2023)018

1. Introduction

Radio-loud Active Galactic Nuclei (AGN) are associated with relativistic jets, which are collimated outflows powered by accretion onto a supermassive black hole (SMBH) [1]. Blazars are a class of jet-dominated (radio loud) AGN in which one of the jets is closely aligned with the observer's line of sight, thus leading to strong Doppler boosting of the observed emission [2]. Blazars are some of the universe's most energetic objects and they radiate across a broad portion of the electromagnetic spectrum.

The optical emission observed from blazars is a combination of thermal emission produced by the accretion disc, broad line region and dusty torus, and non-thermal synchrotron emission produced in the jet, on parsec scales from the SMBH [3]. Studies, such as those done by the RoboPol Collaboration,[1] indicate that blazars exhibit variability in both their emission and linear polarization (e.g. [4]). Radio observations of the parsec scale jets, for example those of the MOJAVE (Monitoring Of Jets in Active galactic nuclei with VLBA Experiments) project,[2] have been able to resolve a large portion of the inner jet structure (e.g. [5], [6]).

Relativistic magneto-hydrodynamic (RMHD) simulations of the sub-parsec and parsec scale jets have been used to explore the jet kinematics and possible causes of variability in the emission and polarization (e.g. [7], [8], [9]). In this study a multi-zone 3D RMHD simulation was employed to reproduce the jet emission and polarization. A two-component spine-sheath model was utilized due to the empirical evidence supporting notable radial velocity structure in relativistic jets (for further details see e.g. [9], [10]).

2. Relativistic Magneto-Hydrodynamic Simulation Setup

A RMHD simulation, consisting of a static grid containing 300×300×600 cells, was constructed using a version of the PLUTO code[3] (ver 4.4; [11], [12]) modified to include Lagrangian particles. A spine-sheath jet model was initially set up on the grid, where the spine had a radius of 10 computational units (0.033 pc) from the centre of the jet and an initial bulk Lorentz factor of $\Gamma = 10$, while the sheath had a radius of 30 computational units (0.1 pc) from the centre of the jet and an initial bulk Lorentz factor of $\Gamma = 3.$. The jet direction was set to be along the z-axis. The pressure ratio of the spine to sheath was set to 1.5, to produce an over-pressurised spine. The jet density was chosen such that the spine and sheath had density ratios relative to the ambient medium of 10^{-3} and 10^{-2}, respectively. Our choice was based on the parsec scale jet model given in [7]. A helical magnetic field with a constant magnetic pitch angle of $\theta_B = 45°$ in the grid reference frame was set up using the same profile used in [9], which is given by,

$$B_\phi = \begin{cases} B_{\phi,\text{spine}} \left(\frac{R}{R_{\text{spine}}}\right)^{\alpha_{\text{spine}}/2}; & \text{if } 0 \le R < R_{\text{spine}} \\ B_{\phi,\text{sheath}} \left(\frac{R}{R_{\text{spine}}}\right)^{\alpha_{\text{sheath}}/2}; & \text{if } R_{\text{spine}} \le R \le R_{\text{sheath}} \\ 0; & \text{if } R > R_{\text{sheath}} \end{cases} \tag{1}$$

[1] http://robopol.physics.uoc.gr
[2] https://www.cv.nrao.edu/MOJAVE/
[3] http://plutocode.ph.unito.it

Parameter:	**Spine:**	**Sheath:**
Toroidal magnetic field parameter(B_ϕ)	50 mG	5 mG
Lorentz factor (Γ)	10	3
Pressure ratio (η_p)	1.5	1.0
Pitch profile parameter (α)	0.5	−2.0

Table 1: Parameters used for the preliminary RMHD jet simulation.

where $B_{\phi,\text{spine}}$ and $B_{\phi,\text{sheath}}$ are the toroidal magnetic field parameters of the spine and the sheath, and R_{spine} and R_{sheath} are the radii of the spine and sheath, respectively. We fixed the pitch profile para exponent, α, in the magnetic field profile to be 0.5 for the spine and −2.0 for the sheath. These values were chosen such that the magnetic pitch increases radially in the spine and decreases in the sheath. A hyperbolic tangential smoothing function was used at the intersections to ensure a smooth transition between the two profiles.

Table 1 contains the simulation parameters that were chosen. For the simulation we chose a rigid numerical scheme consisting of a linear interpolation method, second order Runge-Kutta (RK2) time stepping, and Harten, Lax and van Leer (HLL) Riemann solver.

3. Emission Modelling

Lagrangian particles were created at the base of the jet with random x and y coordinates, within the jet radius, which subsequently propagate with the fluid. Each Lagrangian particle was assigned a power-law energy distribution that represents an ensemble of non-thermal electrons, given by, $N'(E') = N_0\gamma^{-p}$ where p is the spectral index and N_0 is a normalization constant. For our initial spectrum we set $p = 2.8$ and we restrict the power-law distribution to between $\gamma_{\text{min}} = 10^2$ and $\gamma_{\text{max}} = 10^5$. In total 105132 particles were injected into the simulation, which was allowed to evolve until particles were present throughout the jet. The synchrotron, J_{syn}, and linear polarisation, J_{pol}, emission coefficients were calculated during runtime by PLUTO as described in [12]. The emission coefficients were then integrated along the jet beam direction to produce the I, Q and U Stokes parameters given by,

$$I_\nu(\nu, X, Y) = \int_{-\infty}^{\infty} J_{\text{syn}}(\nu, X, Y, Z)dZ, \tag{2}$$

$$Q_\nu(\nu, X, Y) = \int_{-\infty}^{\infty} J_{\text{pol}}(\nu, X, Y, Z)\cos(2\chi)dZ, \tag{3}$$

$$U_\nu(\nu, X, Y) = \int_{-\infty}^{\infty} J_{\text{pol}}(\nu, X, Y, Z)\sin(2\chi)dZ, \tag{4}$$

where χ is the polarization angle as shown in [12]. The relativistic transformations were taken into account before integration. The linear polarization fraction in our simulation was calculated using,

$$\Pi = \frac{\sqrt{Q_\nu^2 + U_\nu^2}}{I_\nu}. \tag{5}$$

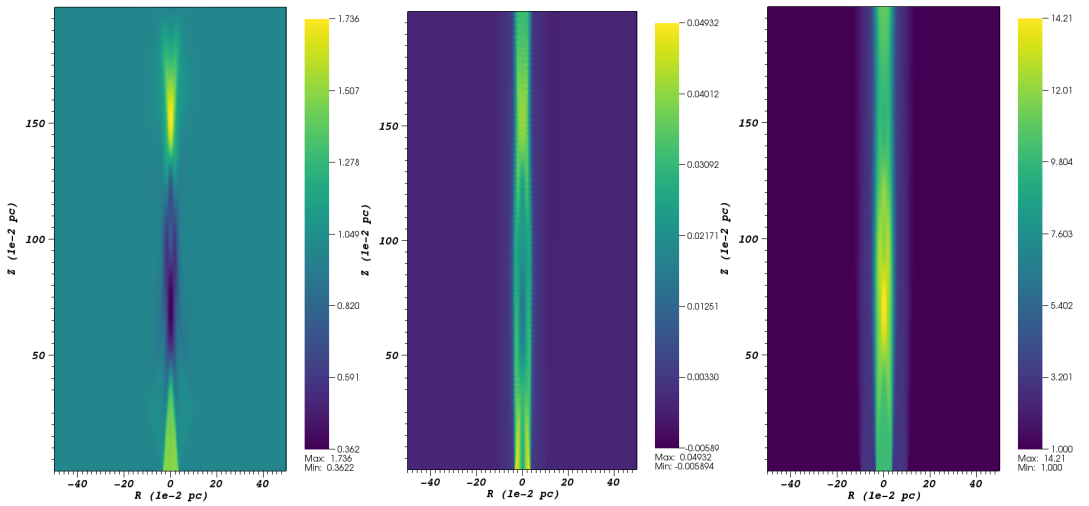

(a) **(b)** **(c)**

Figure 1: The x-z plane sliced along the y-axis to produce 2D images of (a) the pressure, (b) the magnetic field strength and (c) the Lorentz factor of the RMHD simulation. The pressure and magnetic field strength are given in units of dyne/cm^2 and Gauss (G) respectively.

4. Results and Discussion

The pressure, magnetic field and Lorentz factor distributions produced by the simulation are visualized as 2D slices of the x-z plane along the y-axis in figure 1. The jet remains well collimated, showing minimal entrainment of the external medium. Due to the over-pressurised spine being injected into the ambient medium, the spine oscillates as a result of pressure imbalances, leading to the formation of a recollimation pattern. The pressure ratio across the recollimation shock is approximately 1.736, indicating the presence of a weak recollimation shock. The bulk Lorentz factor in the spine of the jet increases to a maximum of 14 due to the expansion and contraction of the spine in the low-pressure region after the first recollimation shock. The Lorentz factor distribution indicates the jet remains highly relativistic across the simulation.

Figure 2 shows the emission coefficients of the simulation at radio (10^8 Hz) and optical (10^{14} Hz) frequencies. Since the synchrotron cooling time decreases with energy ($t_{\text{sync}} \propto 1/E$), the higher energy electrons radiate more quickly, shifting the cutoff energy to lower levels as the electrons cool. This effect influences the emission cutoff, leading to regions where the radio emission remains significant but the optical emission does not.

The modelled intensity was integrated along the length of the jet beam in order to produce a spectral energy distribution (SED) for a simulated object at an arbitrarily selected distance of 324 Mpc. The simulated SED (black points in figure 3a), with a peak at approximately 10^{14} Hz, is consistent with intermediate-frequency peaked BL-Lac (IBL) type blazars [13]. The linear polarization fraction is illusutrated by the blue triangles in figure 3a. Figure 3b shows the linear polarization fraction for a simulated observation from above the jet. The electric vector position angle (EVPA) was overplotted as black bars. The observed EVPA is due to the projection of the magnetic field component which is perpendicular to the line of sight of the observer. Therefore,

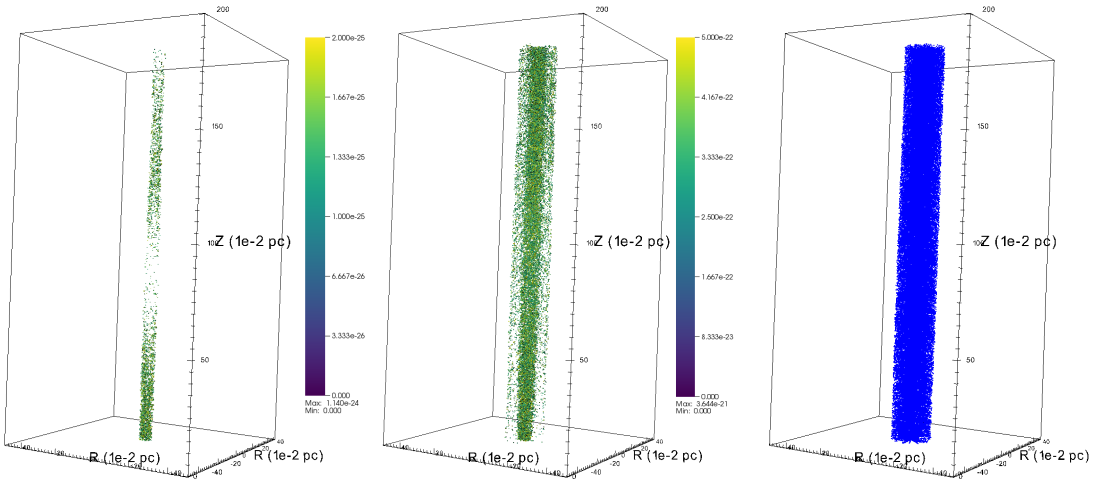

(a) **(b)** **(c)**

Figure 2: (a) The optical (10^{14} Hz) emission coefficient with the threshold limit set to 2×10^{-25} erg s^{-1} cm^{-3} Hz^{-1}, (b) the radio emission coefficient (10^{8} Hz) with the threshold limit set to 5×10^{-22} erg s^{-1} cm^{-3} Hz^{-1} and (c) the distribution of the Lagrangian particles in the jet.

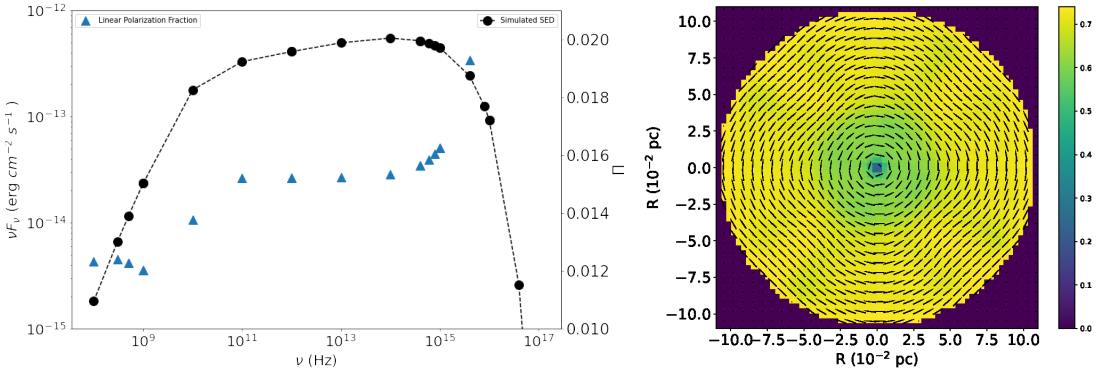

(a) **(b)**

Figure 3: (a) The spectral energy distribution (black points) and the linear polarization fraction (blue points), calculated for an observer along the z-axis. (b) A map of the linear polarization fraction from the beam, projected for an observer along the z-axis. The bars indicate the electric vector position angle (EVPA).

when integrated over the image, a low level of polarization (blue triangles in figure 3a) is found due to the opposite polarization directions cancelling out (e.g [14]). The spine of the jet has a slightly lower polarization fraction than the sheath due to its stronger magnetic field, resulting in a higher rate of particle cooling.

5. Conclusion

A 3D numerical simulation of a magnetized relativistic jet model was created and evolved with time using the PLUTO code. The simulation shows a simple steady state jet, which remains highly relativistic over the domain, with a helical magnetic field morphology and an over pressured

spine that results in the formation of weak recollimation shocks. The 3D simulation shows that we are able to model/simulate the regions that produce emission as well as illustrate that the optical and radio emission arise from different regions. Using the Lagrangian particle module, we were able to reproduce an SED with polarization for a relativistic magnetized spine-sheath jet model. The modelled SED, with a peak at 10^{14} Hz, is comparable to observations of IBL type blazars [13]. The total linear polarization fraction is lower than typically shown in both optical and radio observations by MOJAVE and the Very Long Baseline Array (VLBA) [14]. Possible causes include non-zero alignment of a portion of the jet structure and the presence of a more complex jet structure influencing the polarization fraction. In future work we plan to investigate arbitrary observational angles, in addition to 0°, and analyse the effect on the emission and polarization. We also plan to incorporate a variable jet injection rate to evaluate how the resulting change in jet structure influences the emission and polarization.

References

[1] P. Padovani et al., *Active galactic nuclei: what's in a name?*, *AAR* **25** (2017) 2.

[2] H.M. Schutte, R.J. Britto, M. Böttcher, B. van Soelen, J.P. Marais, A. Kaur et al., *Modeling the Spectral Energy Distributions and Spectropolarimetry of Blazars—Application to 4C+01.02 in 2016–2017*, *ApJ* **925** (2022) 139.

[3] J. Torrealba, T.G. Arshakian, V. Chavushyan and I. Cruz-González, *Correlations between radio emission of the parsec-scale jet and optical nuclear emission of host AGN*, in *Revista Mexicana de Astronomia y Astrofisica Conference Series*, vol. 40 of *Revista Mexicana de Astronomia y Astrofisica Conference Series*, pp. 98–99, Oct., 2011, DOI [1104.2092].

[4] D. Blinov, S. Kiehlmann, V. Pavlidou, G.V. Panopoulou, R. Skalidis, E. Angelakis et al., *RoboPol: AGN polarimetric monitoring data*, *MNRAS* **501** (2020) 3715.

[5] A.B. Pushkarev, H.D. Aller, M.F. Aller, D.C. Homan, Y.Y. Kovalev, M.L. Lister et al., *MOJAVE - XX. Persistent linear polarization structure in parsec-scale AGN jets*, *MNRAS* **520** (2023) 6053 [2209.04842].

[6] M.L. Lister, D.C. Homan, K.I. Kellermann, Y.Y. Kovalev, A.B. Pushkarev, E. Ros et al., *Monitoring Of Jets in Active Galactic Nuclei with VLBA Experiments. XVIII. Kinematics and Inner Jet Evolution of Bright Radio-loud Active Galaxies*, *ApJ* **923** (2021) 30.

[7] G. Fichet de Clairfontaine, Z. Meliani, A. Zech and O. Hervet, *Flux variability from ejecta in structured relativistic jets with large-scale magnetic fields*, *AAP* **647** (2021) A77.

[8] A. Fuentes, J.L. Gómez, J.M. Martí and M. Perucho, *Total and Linearly Polarized Synchrotron Emission from Overpressured Magnetized Relativistic Jets*, *ApJ* **860** (2018) 121.

[9] Z. Meliani and R. Keppens, *Decelerating Relativistic Two-Component Jets*, *ApJ* **705** (2009) 1594 [0910.0332].

[10] P.E. Hardee, *Stability Properties of Strongly Magnetized Spine-Sheath Relativistic Jets*, *ApJ* **664** (2007) 26.

[11] A. Mignone, G. Bodo, S. Massaglia, T. Matsakos, O. Tesileanu, C. Zanni et al., *PLUTO: A Numerical Code for Computational Astrophysics*, *ApJ* **170** (2007) 228.

[12] B. Vaidya, A. Mignone, G. Bodo, P. Rossi and S. Massaglia, *A Particle Module for the PLUTO Code. II. Hybrid Framework for Modeling Nonthermal Emission from Relativistic Magnetized Flows*, *ApJ* **865** (2018) 144.

[13] A.A. Abdo, M. Ackermann, I. Agudo, M. Ajello, H.D. Aller, M.F. Aller et al., *The Spectral Energy Distribution of Fermi Bright Blazars*, *ApJ* **716** (2010) 30.

[14] M.L. Lister, M.F. Aller, H.D. Aller, M.A. Hodge, D.C. Homan, Y.Y. Kovalev et al., *MOJAVE. XV. VLBA 15 GHz Total Intensity and Polarization Maps of 437 Parsec-scale AGN Jets from 1996 to 2017*, *ApJ* **234** (2018) 12.